A study of uniaxial and constant-width drawing of poly(ethylene terephthalate)

D. H. Gordon, R. A. Duckett and I. M. Ward*

IRC in Polymer Science and Technology, University of Leeds, Leeds LS2 9JT, UK

(Received 20 October 1993; revised 14 December 1993)

The two-stage drawing of uniaxially oriented poly(ethylene terephthalate) (PET) films has been undertaken, together with the drawing of films at constant width, which are biaxially oriented, under equivalent conditions of temperature and strain rate. From measurements of the changes in refractive index, drawing stress and peak shrinkage stress, it is concluded that the behaviour can in all cases be described by the deformation of a molecular network, which is of a very similar nature not only for all these present measurements but also for previous studies of PET fibres and films.

(Keywords: poly(ethylene terephthalate); drawing; films)

INTRODUCTION

It has long been recognized that the concept of a deforming molecular network can be very valuable in understanding the development of molecular orientation in poly(ethylene terephthalate) (PET) fibres and films during melt spinning and tensile drawing processes. Previous research on this subject includes stress-optical measurements on spun fibres[1] and hot-drawn films[2], studies of molecular reorientation in deformation bands[3] and, more recently, attempts to relate the properties of fibres produced by two-stage high speed spinning/hot drawing to a 'network draw ratio' determined by matching load–elongation curves[4]. There is also a substantial body of work on the characterization of molecular orientation by i.r., and Raman and polarized fluorescence spectroscopy, which relates the development of orientation and changes in molecular conformation to the deformation of an idealized molecular network of equivalent random links[5–7].

The research described above has been concerned almost entirely with fibres or with films developing uniaxial orientation. In this paper we describe the two-stage drawing of uniaxially oriented PET films and the drawing of samples at constant width which are biaxially oriented. A principal aim of this work has been to examine whether a similar molecular network can be considered to exist and to be preserved in this range of drawing processes, providing that they are undertaken under equivalent conditions of temperature and strain rate. To test this proposal we have combined measurements of the refractive indices of drawn films with measurements of the drawing stress and of the peak shrinkage stress which develops when the drawn film is held at constant length at a temperature just above the glass transition temperature T_g.

THEORY

The theory for the stress-optical behaviour of rubbers was first developed by Kuhn and Grün[8] for uniaxial deformation. There are two key equations. First, the tensile stress σ produced by the uniaxial extension of a rubber network to an extension ratio λ is given by:

$$\sigma = N_0 kT(\lambda^2 - \lambda^{-1}) \tag{1}$$

where k is the Boltzmann constant, T is the absolute temperature and N_0 is the number of chains per unit volume. Similarly, the optical anisotropy is given by the birefringence:

$$\Delta n = \frac{2\pi}{45}\frac{(\bar{n}^2+2)^2}{\bar{n}} N_0(\alpha_1 - \alpha_2)(\lambda^2 - \lambda^{-1}) \tag{2}$$

where $\bar{n}$ is the mean refractive index, α_1 is the polarizability of the random link along its length direction, and α_2 is the mean polarizability in a transverse direction.

From equations (1) and (2) the stress-optical coefficient $\Delta n/\sigma$ is given by:

$$\frac{\Delta n}{\sigma} = \frac{2\pi}{45kT}\frac{(\bar{n}^2+2)^2}{\bar{n}}(\alpha_1 - \alpha_2) \tag{3}$$

Measurements of the variation of stress σ with extension ratio λ allow the degree of crosslinking of the network in terms of N_0 to be obtained from equation (1). The stress-optical coefficient enables a determination of the principal polarizability difference for the random link $(\alpha_1 - \alpha_2)$ from equation (3), and if the optical anisotropy of the monomer unit can be calculated, then the number of monomer units per equivalent random link can be determined. In this paper we have used the values for the optical anisotropy of the monomer unit given in previous work[1].

A very instructive way of presenting the refractive index data for a more general deformation to extension ratios λ_1, λ_2 and λ_3 has been given by Treloar[9]. He showed that the refractivity $(n^2-1)/(n^2+2)$ is given by:

$$\frac{n_1^2-1}{n_1^2+2} = \frac{4\pi N_0}{3}[(n/3)(\alpha_1+2\alpha_2) + \frac{1}{15}(\alpha_1-\alpha_2)(2\lambda_1^2 - \lambda_2^2 - \lambda_3^2)] \tag{4}$$

* To whom correspondence should be addressed

0032-3861/94/12/2554-06

with similar equations for n_2 and n_3, n being the number of random links per chain. This equation allows data from uniaxially and biaxially drawn materials to be compared directly and allows an independent check on the values for N_0 and $(\alpha_1 - \alpha_2)$ to be obtained.

EXPERIMENTAL

Preparation of isotropic samples

ICI Films, Wilton, provided two rolls of isotropic amorphous film of approximately 500 μm and 200 μm thickness. This film was produced by melt extrusion onto a chilled roller. The intrinsic viscosity of the film was 0.6, which corresponds to a number average molecular weight of about 2×10^5.

Uniaxial drawing

Dumbbell samples of isotropic film with initial dimensions 100 mm × 2 mm × 0.2 mm were drawn on an Instron tensile testing machine at a range of temperatures around T_g (70–90°C) with constant cross-head speeds ranging from 0.1 to 10 cm min^{-1}. After drawing, the samples were held in the Instron and rapidly cooled to room temperature.

For two-stage uniaxial drawing, strip samples of length 50 mm were cut from uniaxially drawn films which had been prepared with a range of draw ratios by drawing at 80°C at 10 cm min^{-1} cross-head speed from dumbbells of size 100 mm × 2 mm × 0.5 mm. These samples were redrawn to similar final draw ratios at 5 cm min^{-1} cross-head speed (i.e. equivalent initial strain rate), also at 80°C.

Constant-width drawing

Samples were drawn at constant width at 85°C using either a commercial Bruckner biaxial stretching machine or a specially built stretching facility which could also be used to measure both the drawing stress and the shrinkage stress. For drawing in the specially built facility, 13.8 cm × 8.5 cm × 0.2 mm samples were clamped at constant width to give a gauge length of 4 cm, and were drawn in the direction perpendicular to the 8.5 cm dimension at a cross-head speed of 4.38 cm min^{-1} in a silicone–oil bath, to give comparability with samples drawn uniaxially on the Instron machine.

Density measurements

The densities of all the films were measured using density gradient columns based on two aqueous solutions of potassium iodide covering the range 1.25–1.45 g cm^{-3}.

Refractive index measurements

The refractive indices of the films were measured using either an Abbe refractometer or an interference microscope, as will be indicated in the Results section.

Shrinkage stress measurements

Shrinkage force measurements were made on uniaxially drawn film using an apparatus which has been extensively used in our laboratories for such measurements on oriented fibres and tapes[10]. In this case samples 6 cm long by 2 mm wide were held at constant length and then immersed in a silicone oil bath at 88°C. The initial peak value of the force which resulted was used to calculate the shrinkage stress.

For shrinkage stress measurements on films drawn at constant width the instrumented custom-built drawing facility was used. After drawing at 80°C the sample was removed from the oil bath and left to cool to room temperature, whilst held at constant length in the clamps. It was then re-immersed in the oil bath, which had reached equilibrium at 88°C, and the peak value of the shrinkage force was recorded.

RESULTS

Uniaxial drawing

Redrawing. True stress–strain curves are shown in *Figure 1* for the second drawing of samples which had previously been drawn to a range of initial draw ratios up to 5 and then redrawn to similar final draw ratios. It can be seen that at high draw ratios the stress–strain curves show a rapid strain hardening. This occurs at lower values of second draw ratio λ_2 for samples that had a high initial draw ratio λ_1. Individual stress–strain curves in *Figure 1* may be shifted along the log (draw ratio) axis to produce optimum superposition of the strain-hardening regions; the shift factors $A(\lambda_1)$ required are shown in *Figure 2* plotted as $\log_e A$ *versus* $\log \lambda_1$. The slope of the line, which is a least-squares best fit, is 1.025 implying that the effective draw ratio, $\lambda_e = \lambda_2 A(\lambda_1)$, is indeed very close to the total draw ratio, $\lambda_F = \lambda_2 \lambda_1$. *Figure 3* shows the curves of stress plotted *versus* $\log_e(\lambda_e) = \log_e(A\lambda_2)$, and it can be seen that there is excellent superposition in the strain-hardening regions of the stress–strain curves.

Comparisons of the birefringence (using interference microscopy) and density data obtained from single-stage and two-stage uniaxially drawn film plotted as a function of both λ and λ_F are made in *Figures 4* and *5*, respectively. The observation that the birefringence, density and shrinkage stress depend only on total draw

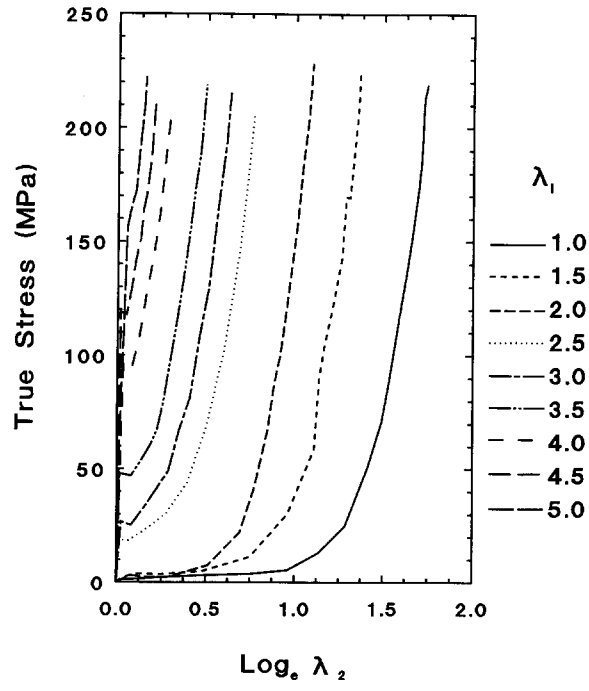

Figure 1 True stress *versus* $\log_e$(draw ratio) curves for the redrawing of samples of PET which had been predrawn to the indicated draw ratio (λ_1). Both drawing stages were uniaxial at 80°C; initial strain rate 3.3×10^{-3} s^{-1} in each case

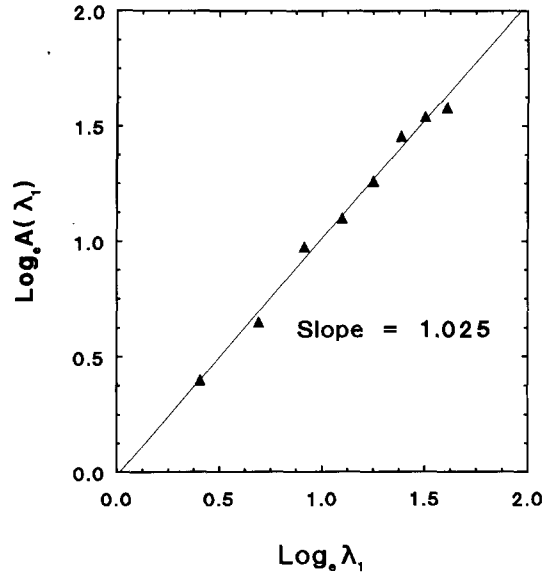

Figure 2 The horizontal shift factors needed to superpose the high stress regions of the curves from *Figure 1*. The unit gradient implies that the shift factor $A(\lambda_1)$ is approximately equal to the initial draw ratio λ_1

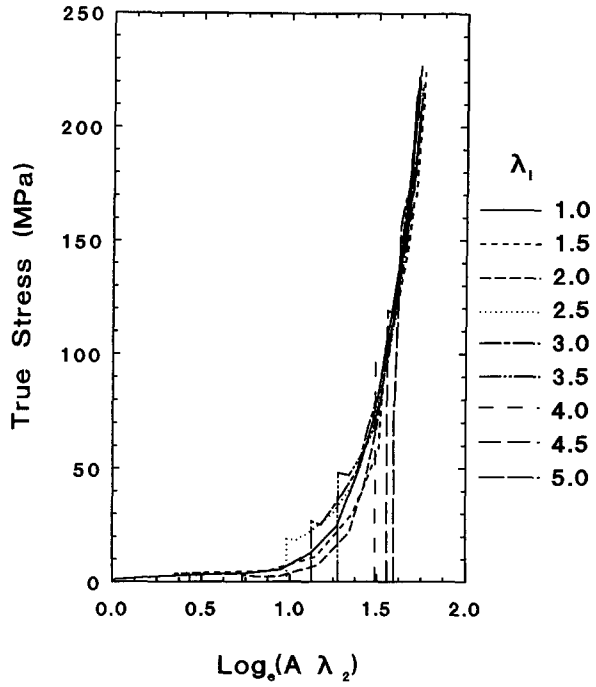

Figure 3 'Master curves' showing the superposition of individual stress–strain curves from *Figure 1* shifted according to the factors $A(\lambda_1)$ shown in *Figure 2* (A = shift factor $\approx \lambda_1$)

ratio lends support to the idea that there is a molecular network which is preserved throughout the drawing process at 80°C.

Strain rate and temperature dependence. Figure 6 shows a plot of the draw stress at a uniaxial draw ratio of 3.0 *versus* log(initial strain rate/s^{-1}) at four drawing temperatures around T_g. It can be seen that the strain-rate dependence is a maximum at 80°C and is insignificant at higher or lower temperatures. Unpublished work[11] has shown that the shrinkage stress and birefringence values for samples uniaxially drawn to a draw ratio of

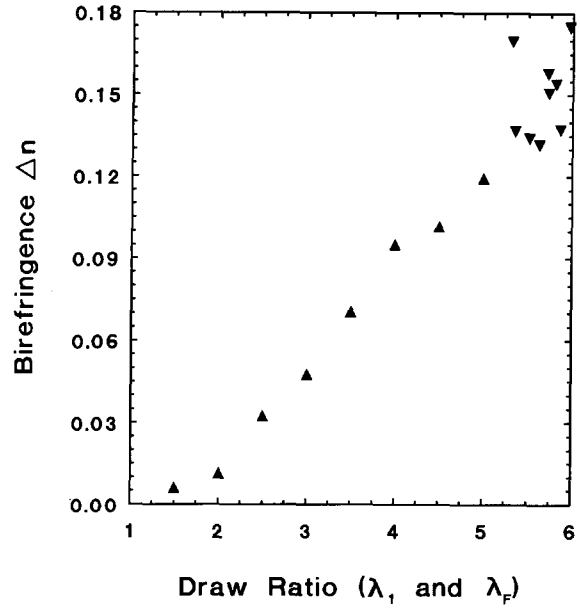

Figure 4 Birefringence *versus* final draw ratio for PET samples drawn in a single stage (▲) or in two stages (▼)

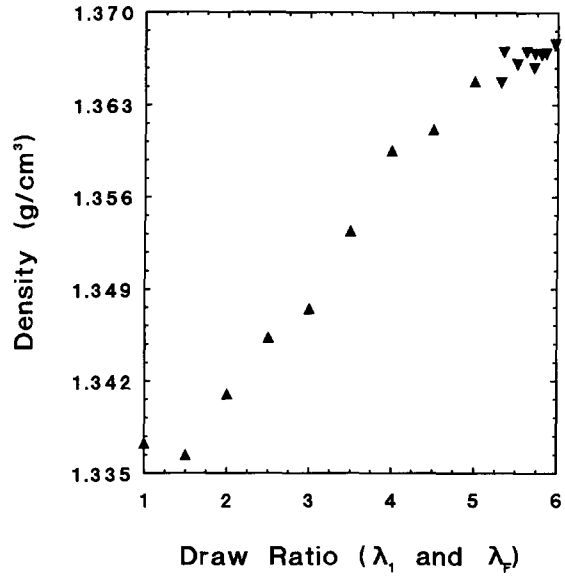

Figure 5 Density *versus* final draw ratio for PET samples drawn in a single stage (▲) or in two stages (▼)

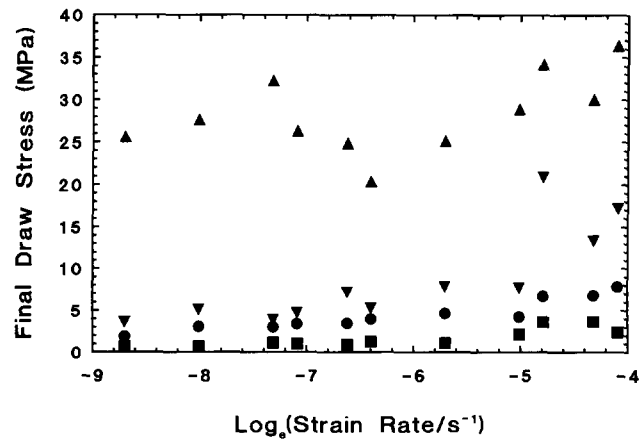

Figure 6 The strain-rate dependence of the draw stress at a draw ratio of 3.0 for samples uniaxially drawn at 70°C (▲), 80°C (▼), 85°C (●) and 90°C (■)

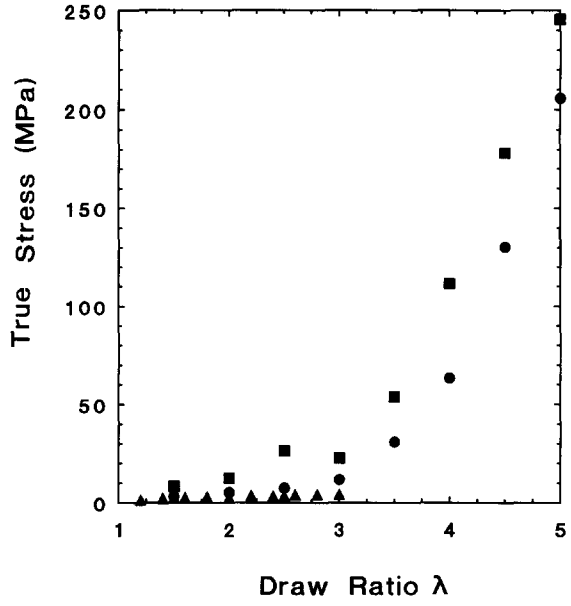

Figure 7 True stress *versus* draw ratio for PET uniaxially drawn at 75°C (■), 80°C (●) and 85°C (▲) (initial strain rate $6.7 \times 10^{-3}\,s^{-1}$)

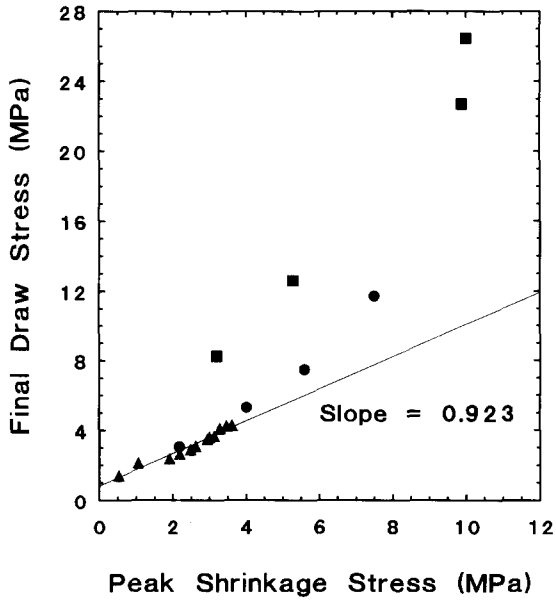

Figure 8 Final draw stress *versus* peak shrinkage stress (see text) for PET samples uniaxially drawn at 75°C (■), 80°C (●) and 85°C (▲). The straight line is a best fit to the data from drawing at 85°C, indicating that at this temperature the main component of the drawing stress is the entropic stress in the molecular network

3.0 at 80°C are also independent of strain rate. The true stress *versus* draw ratio curves for uniaxial drawing at a strain rate of $0.0067\,s^{-1}$ at three different temperatures are shown in *Figure 7*. The increase in strain hardening at draw ratios above 2.5 is probably an indication of strain-induced crystallization, as discussed further below.

Shrinkage stress. Figure 8 shows a comparison between the final draw stress and the shrinkage stress for samples drawn at an initial strain rate of $0.0067\,s^{-1}$ at temperatures of 75, 80 and 85°C. The full line has a slope of 0.923 and indicates that for samples drawn at 85°C the shrinkage stress is equal to the drawing stress to a good approximation, whereas at lower temperatures the draw stress exceeds the shrinkage stress by a considerable margin. It is believed that the intercept on this graph represents a small but significant contribution from the internal viscosity to the drawing stress.

Constant width drawing

A comparison of the densities of films drawn uniaxially and at constant width (initial strain rate $0.0067\,s^{-1}$ at 85°C) is made in *Figure 9*. It can be seen that there is little evidence of crystallization at draw ratios less than 2.5 in both types of drawing. The further observation in uniaxial drawing, that the drawing stress at 85°C and the shrinkage stress are very similar, supports the idea that it is fruitful to make a comparison of these types of drawing under these conditions.

On the assumption, therefore, that both uniaxial and constant-width drawing involve stretching of an identical molecular network, the following points can be made. First, the network stress (either the drawing or shrinkage stress) should relate to the network draw ratio, most simply on the basis that the free energy change is entirely entropic. Thus if

$$F = \text{const}(\lambda_1^2 + \lambda_2^2 + \lambda_3^2 - 3)$$

then

$$\sigma_{\text{uniaxial}} \propto (\lambda^2 - \lambda^{-1})$$

and

$$\sigma_{\text{constant width}} \propto (\lambda^2 - \lambda^{-2})$$

This comparison is illustrated in *Figures 10* and *11* where the drawing and shrinkage stresses are compared for the two types of drawing. It can be seen that: (i) there is very good agreement between the two sets of data; and (ii) the correlation between draw stress and shrinkage stress is established for both uniaxial and constant-width drawing. This suggests that there is a negligible viscosity contribution to the drawing stress under these conditions.

Secondly, there should be a unique relationship between the shrinkage stress and the birefringence, i.e. a constant stress-optical coefficient. This is confirmed

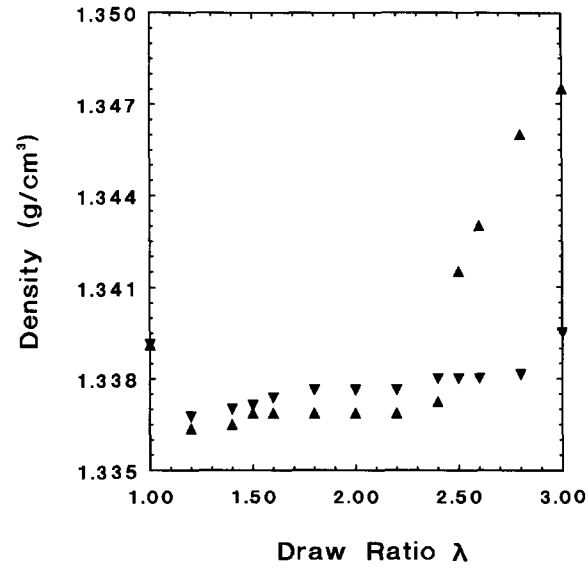

Figure 9 Comparison of the density of PET film drawn uniaxially (▲) or at constant width (▼) at 85°C. Note the delayed onset of crystallization in the constant-width film

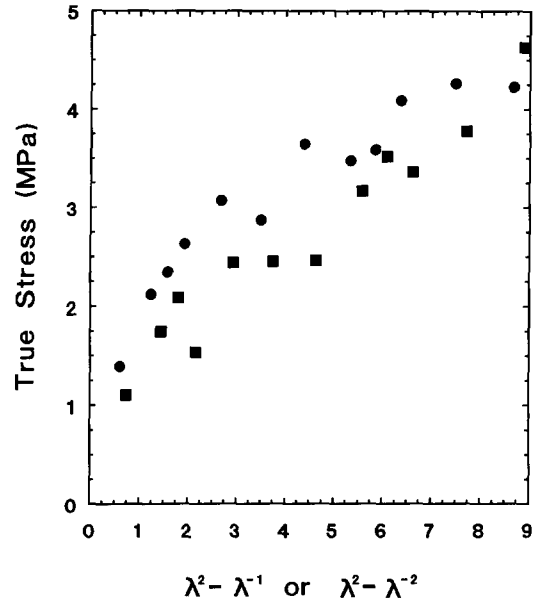

Figure 10 Variation of drawing stress with the appropriate Gaussian parameter for PET film drawn uniaxially (●) or at constant width (■) at 85°C. Note the approximate equivalence between these two data sets

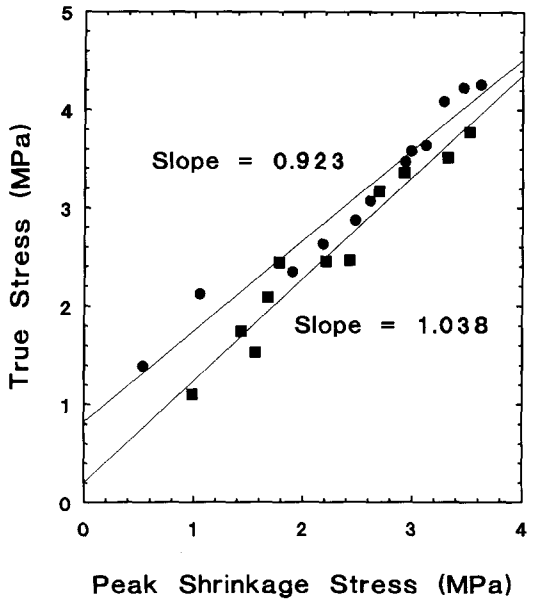

Figure 11 Draw stress *versus* peak shrinkage stress (see text): comparison of uniaxial (●) and constant width (■) materials drawn at 85°C

by the correlation shown in *Figure 12*, where the birefringence refers to the difference in refractive index for light travelling with the electric vector parallel to either the draw direction or the thickness direction, measured by the Abbe refractometer. Closer inspection of the data by examining the relationship between birefringence and the appropriate strain parameter (*Figure 13*) does suggest that there is a divergence between results for uniaxial and constant-width samples at high draw ratios, which can be attributed to the onset of crystallization in the uniaxial samples. Note that the appropriate birefringence for this comparison is the difference in refractive indices in the draw direction and parallel to the sheet normal, as has been plotted here.

Following the theoretical treatment of Treloar[9] (equation (4)), the combined results for the two types of drawing are shown in *Figure 14*, where $(n_i^2-1)/(n_i^2+2)$ is plotted against either $(2\lambda_i^2-2\lambda_i^{-1})$ or $(2\lambda_i^2-1-\lambda_i^{-2})$ for uniaxial or constant width samples, respectively. Note that this graph contains data for refractive indices n_3 in the direction of draw and n_1 and n_2 in the two perpendicular directions for the constant-width samples. It can be seen that there is excellent overall agreement between results for all refractive indices for the two different drawing processes.

DISCUSSION

The comparison of drawing stress, shrinkage stress and refractive index measurements, for the samples drawn

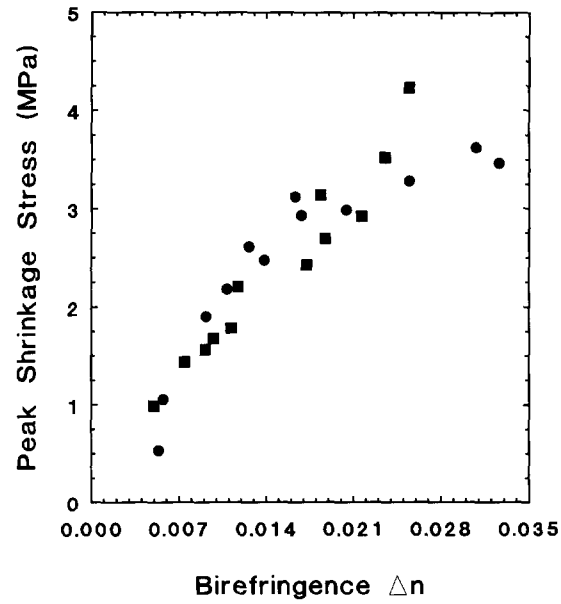

Figure 12 Peak shrinkage stress (see text) *versus* birefringence: comparison of uniaxial (●) and constant width (■) materials drawn at 85°C. (Note: the birefringence measured is the difference in refractive indices parallel to the draw direction and thickness direction)

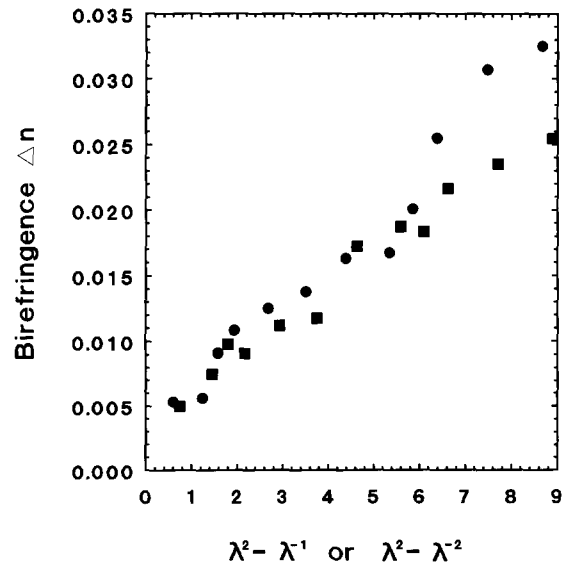

Figure 13 Variation of birefringence with the appropriate Gaussian parameter for uniaxial (●) and constant width (■) materials drawn at 85°C

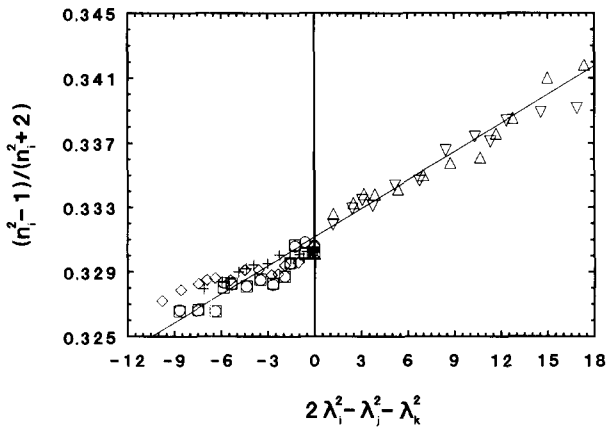

Figure 14 Refractivity data for uniaxial and constant-width materials. Uniaxial: Δ, n_3; □, n_1; ○, n_2. Constant width: ▽, n_3; +, n_1; ◇, n_2 (the index 3 is in the draw-direction, 1 is in the thickness direction)

uniaxially and at constant width, suggests that drawing of PET under comparable conditions of temperature and strain rate at 85°C can be very well described as the deformation of a molecular network. The stress-optical coefficient extracted from *Figure 12* indicates values for $\alpha_1-\alpha_2$ in the range $(1.32–1.63)\times10^{-29}\,m^{-3}$, which compare with a value of $1.51\times10^{-29}\,m^{-3}$ from similar measurements on melt-spun PET fibres by Pinnock and Ward[1], and $1.7\times10^{-29}\,m^{-3}$ on PET films drawn at 80°C by Rietsch *et al.*[2]. The entanglement (or effective crosslink) density can be found from *Figures 10* and *13*, and suggests values in the range $(1.5–2.32)\times10^{26}\,m^{-3}$, which compare with values of $1.8\times10^{26}\,m^{-3}$ (ref. 1) and $1.89\times10^{26}\,m^{-3}$ (ref. 2). The agreement between these different experiments is good and suggests that the molecular network formed is quite similar in all cases. In terms of the Kuhn and Grün[8] random link model, such values corresponds to two to three monomer units per random link, and about seven random links per chain between entanglements.

CONCLUSIONS

1. It has been shown that the drawing behaviour of PET in the temperature range just above T_g can be interpreted in terms of the deformation of a molecular network.
2. The drawing stress is almost identical to the stress generated when the drawn and quenched sample is held at constant length and heated above T_g.
3. The drawing stress at high stresses is essentially determined by the total draw ratio, independent of whether the sample was deformed in a single stage or in a two-stage process.
4. The changes in refractive indices and stress with deformation in this temperature range, in both uniaxial and constant-width deformation, are described approximately by the Gaussian theory of rubber elastic photo-elasticity.

ACKNOWLEDGEMENTS

D. H. Gordon held an SERC CASE studentship sponsored by ICI Films. The authors thank Dr D. P. Jones and Dr D. J. Blundell, of ICI Films, for the supply of materials and for many helpful discussions during the course of the research.

REFERENCES

1 Pinnock, P. R. and Ward, I. M. *Trans. Faraday Soc.* 1966, **62**, 1308
2 Rietsch, F., Duckett, R. A. and Ward, I. M. *Polymer* 1979, **20**, 1133
3 Brown, N., Duckett, R. A. and Ward, I. M. *J. Phys D* 1968, **1**, 1369
4 Long, S. D. and Ward, I. M. *J. Appl. Polym. Sci.* 1991, **42**, 1911
5 Cunningham, A., Ward, I. M., Willis, H. A. and Zichy, V. *Polymer* 1974, **15**, 749
6 Nobbs, J. H., Bower, D. I. and Ward, I. M. *J. Polym. Sci., Polym. Phys. Edn* 1979, **17**, 259
7 Lapersonne, P., Bower, D. I. and Ward, I. M. *Polymer* 1992, **33**, 1277
8 Kuhn, W. and Grün, F. *Kolloid Z.* 1942, **101**, 248
9 Treloar, L. R. G. 'The Physics of Rubber Elasticity', 3rd Edn, Clarendon Press, Oxford, 1975
10 Capaccio, G. and Ward, I. M. *Colloid Polym. Sci.* 1982, **260**, 46
11 Gordon, D. H. PhD Thesis, Leeds University, 1992